
Conformalized Online Learning: Online Calibration Without a Holdout Set

Shai Feldman

Department of Computer Science
Technion, Israel

shai.feldman@cs.technion.ac.il

Stephen Bates

Departments of Statistics and of EECS
UC Berkeley

stephenbates@cs.berkeley.edu

Yaniv Romano

Departments of Electrical and Computer Engineering
and of Computer Science
Technion, Israel

yromano@technion.ac.il

Abstract

We develop a framework for constructing uncertainty sets with a valid coverage guarantee in an online setting, in which the underlying data distribution can drastically—and even adversarially—shift over time. The technique we propose is highly flexible as it can be integrated with any online learning algorithm, requiring minimal implementation effort and computational cost. A key advantage of our method over existing alternatives—which also build on conformal inference—is that we do not need to split the data into training and holdout calibration sets. This allows us to fit the predictive model in a fully *online* manner, utilizing the most recent observation for constructing calibrated uncertainty sets. Consequently, and in contrast with existing techniques, (i) the sets we build can quickly adapt to new changes in the distribution; and (ii) our procedure does not require refitting the model at each time step. Using synthetic and real-world benchmark data sets, we demonstrate the validity of our theory and the improved performance of our proposal over existing techniques. To demonstrate the greater flexibility of the proposed method, we show how to construct valid intervals for a multiple-output regression problem that previous sequential calibration methods cannot handle due to impractical computational and memory requirements.

1 Introduction

To confidently deploy learning models in high-stakes applications, we need both high predictive accuracy and reliable safeguards to handle unanticipated changes in the underlying data generating process. Reasonable accuracy on a fixed validation set is not enough [1–5]; we must also quantify uncertainty to correctly handle hard input points and take into account shifting distributions. For example, consider the task of estimating future oxygen saturation levels of a hospitalized patient given past data, such as the patient’s blood pressure, heart rate, body temperature, and more. The doctor must decide which medical treatment should be used for preventing deterioration in the patient’s health condition. Here, providing a point estimate of oxygen saturation for the doctor is insufficient—it does not communicate the range of outcomes for the individual’s medical condition that the doctor needs to carefully weigh the pros and cons of different treatment options [6–8]. In these situations, it is necessary to design a predictive system that reflects the range of plausible outcomes. In this work, we encode uncertainty in a rigorous manner via prediction intervals/sets that augment point predictions. Studies of how people engage with automated systems had shown

that returning prediction sets is an effective way to communicate uncertainty [9]. In this paper, we introduce a novel calibration framework that can wrap any online learning algorithm (e.g., an LSTM model trained online) to construct prediction sets with guaranteed validity.

Formally, suppose an online learning setting where we are given data stream $\{(X_t, Y_t)\}_{t \in \mathbb{N}}$ in a sequential fashion, where $X_t \in \mathcal{X} = \mathbb{R}^p$ is a feature vector and $Y_t \in \mathcal{Y}$ is a target variable. In regression settings $\mathcal{Y} = \mathbb{R}$, while in classification tasks \mathcal{Y} is a finite set of all class labels. At each time step $t \in \mathbb{N}$, we use all samples previously observed $\{(X_i, Y_i)\}_{i=1}^{t-1}$ along with the test feature vector X_t to construct a prediction set $\hat{C}_t \subseteq \mathcal{Y}$, guaranteed to attain any user-specified coverage frequency $1 - \alpha$, e.g., 90%:

$$\lim_{T \rightarrow \infty} \frac{1}{T} \sum_{t=1}^T \mathbb{1}_{\{Y_t \in \hat{C}_t(X_t)\}} = 1 - \alpha. \quad (1)$$

Conformal inference [10–14] is a generic approach for constructing prediction sets with valid coverage, under the assumption that the training and testing points are i.i.d., or exchangeable. Since this assumption is often violated in sequential real-world applications, extensions to conformal inference were developed, which impose relaxed notions of exchangeability [15–20]. These methods, however, are not guaranteed to construct valid prediction sets for time-series data with less regular distributional shifts. By contrast, *adaptive conformal inference* (ACI) [21] is a groundbreaking calibration scheme for constructing prediction sets with valid coverage in the sense of (1) for any arbitrary time-varying data distribution. To attain the nominal coverage rate, this method splits the observed data into a training and holdout calibration set at each time step; the idea is to leverage the holdout points to quantify the prediction uncertainty of the model fitted on the training data. Data splitting has two main drawbacks, however. First, it makes it cumbersome to deploy online learning algorithms, which are computationally efficient. Second, the predictive model cannot be fitted on the most recent data points. The former implies that we must retrain the model from scratch once a new test point is observed, which is computationally inefficient. The latter implies that the model will slowly adapt to changes in the distribution, as it is blind to these recent data points.

In this work, we introduce *rolling conformal inference* (Rolling CI): a novel calibration procedure that addresses the drawbacks of ACI by removing the requirement of a holdout set. Our scheme is guaranteed to attain any pre-specified coverage level without making any assumptions on the data distribution. It can be integrated with any online learning algorithm, and can utilize all the data for training. We will detail the novelty of our proposal below, but first, we turn to present a synthetic experiment demonstrating the advantages of our Rolling CI compared to ACI.

1.1 A Synthetic Example

To illustrate the challenges in constructing prediction intervals with accurate coverage rate, we conduct a synthetic experiment using time-series data with drastic distributional shifts. We generate a response variable $Y_t \in \mathbb{R}$ at time t as follows:

$$Y_t = \frac{1}{2}Y_{t-1} + |\beta_t^T X_t| \omega_t + \varepsilon_t,$$

where X_t is a feature vector of length 5, β_t is a time-varying regression coefficient vector, ω_t is a time-varying scale variable, and ε_t is a noise term. Both ω_t and β_t are updated every 500 steps: the former alternates between 1 and a large random number, and the latter vector is sampled from a uniform distribution. Figure 1a visualizes this synthetic data set—notice how a distributional shift occurs every 500 time steps. The full description of this data is given in Supplementary Section D.1.

Next, we fit a neural network as a base model and a construct prediction interval using ACI and our proposed method, where we set the target coverage level to 90%. In Section B of the Supplementary Material, we give more details regarding the online training setup. To demonstrate the greater adaptivity of our method and the importance of this property, we evaluate the performance of each method across two groups that are identified by ω_t . Specifically, a point (X_t, Y_t) is assigned to group 1 if $\omega_t = 1$ and to group 0 otherwise. Following Figure 1b, we can see that the proposed method not only constructs narrower intervals, but also accurately attains the desired coverage level for each group, in contrast to ACI. Lastly, both ACI and our method achieve valid coverage over the last 2000 samples, 90.01% and 89.95%, respectively.

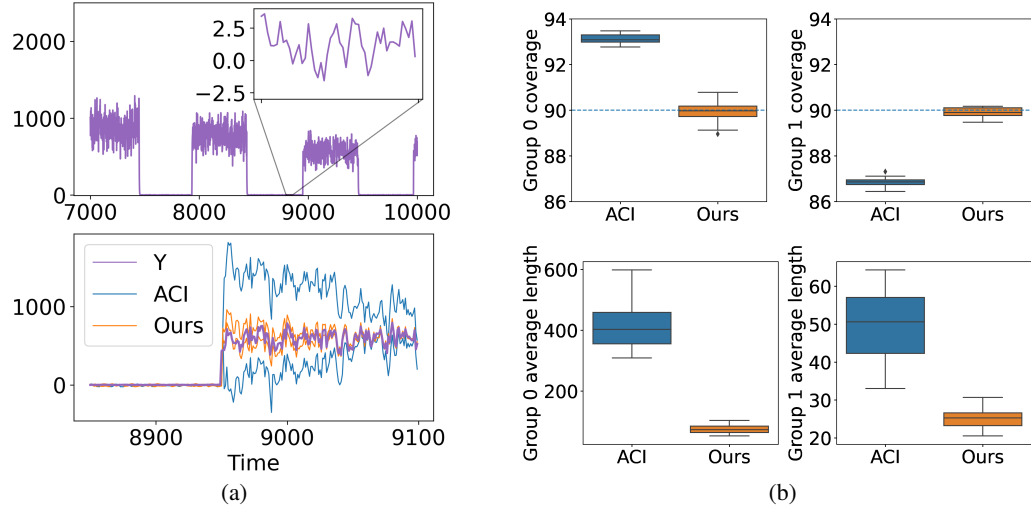


Figure 1: The proposed method quickly adapts to shifts in the distribution. (a) visualization of the response as a function of t (purple) and the intervals constructed with ACI (blue) and with the proposed method (orange) (b) Group-wise coverage (top) and length (bottom) of ACI (blue) and the proposed method (orange). Target coverage level is 90%. The performance metrics are evaluated over 20 independent trials.

1.2 Our contribution

Before formally presenting `Rolling CI`, we pause to state the key features of our proposal.

Valid coverage. Theorem 1 guarantees that our calibration method is guaranteed to satisfy the requirement in (1) for any time-varying data distribution and predictive model.

Faster reaction to distribution shift. In contrast to existing techniques [21, 22], our proposal does not reserve a holdout set for calibrating the prediction interval at each inference step. This allows fitting the model on the entire data stream, and utilizing the most recent observations to better track the underlying distribution. Indeed, the experiments in Section 5, conducted on real benchmark data sets, demonstrate that our method yields more informative prediction sets than existing methods.

Compatibility with online learning models. Our method works together with any black-box online learning algorithm to adaptively control any parameter that encodes the size of the prediction set. Since we avoid costly model refitting, our procedure is more computationally efficient—in Section 5.2, we apply our method to multiple-output regression task where the alternative sequential calibration methods are infeasible.

Software implementing the proposed framework and reproducing our experiments is available at <https://github.com/Shai128/rcl>.

2 Background

In this section, we provide a short description of uncertainty quantification techniques that we build upon. We also explain in details more relevant methods in Supplementary Section E.

2.1 Split Conformal Prediction

Split conformal prediction (SCP) [23] is a general tool for constructing prediction sets in regression or classification tasks. In a nutshell, the idea is to split the observed labeled data $\{(X_i, Y_i)\}_{i=1}^n$ into training and calibration sets, fit a model on the training set, and evaluate the model goodness-of-fit on the reserved holdout calibration points. This goodness-of-fit information is then cleverly used

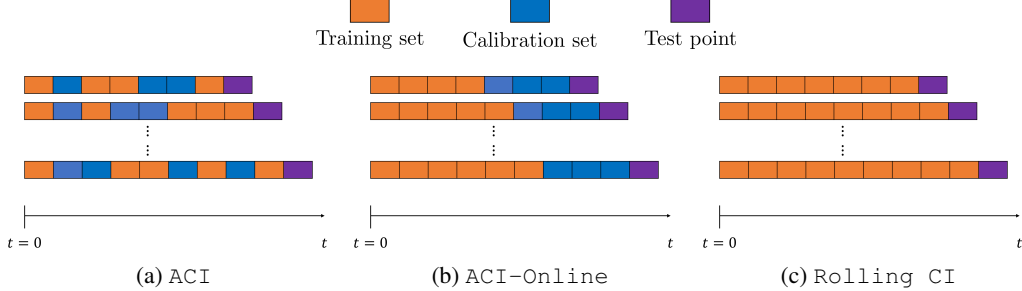


Figure 2: Visualization of the three calibration schemes discussed in this paper.

to assess the uncertainty in future predictions. We provide a detailed description of this method in Section E.1 of the Supplementary Material. Under the assumption that the training and test points are sampled i.i.d. from some unknown distribution P_{XY} , the prediction set $C_{1-\alpha}^{\text{SCP}}(X) \subseteq 2^{\mathcal{Y}}$ constructed via SCP is guaranteed to contain the test target variable Y with probability at least $(1-\alpha)$. Importantly, this coverage guarantee holds on average over the randomness of the training and test points. In particular, this statement does not hold for time-varying data with arbitrary distributional shifts, as the i.i.d. assumption would not hold anymore. This limitation is addressed by the method presented next.

2.2 Adaptive Conformal Inference

Adaptive conformal inference (ACI) [21] is a powerful calibration scheme guaranteed to construct valid prediction sets in the sense of (1) in an online setting, where the underlying distribution can vary greatly over time. Suppose we are given a labeled data stream $\{(X_t, Y_t)\}_{t=1}^{T-1}$ and a new test point X_T with an unknown Y_T . ACI constructs a prediction set for Y_T by invoking SCP as a subroutine, with a carefully tuned target coverage level $1 - \alpha_T$ for the time step T ,

$$C_T^{\text{ACI}}(X_T) = C_{1-\alpha_T}^{\text{SCP}}(X_T). \quad (2)$$

Above, α_T is tuned recursively according to the following rule:

$$\alpha_{T+1} = \alpha_T + \gamma(\alpha - \text{err}_T), \quad \text{where} \quad \text{err}_T = \begin{cases} 1, & Y_T \notin C_T^{\text{ACI}}(X_T), \\ 0, & \text{otherwise,} \end{cases} \quad (3)$$

which ensures that (1) will rigorously hold. Above, $1 - \alpha$ is the desired coverage frequency specified by the user (e.g., 90%) and $\gamma > 0$ is a fixed step size, e.g., 0.05. Intuitively, (3) tracks the empirical long-range coverage rate, and adaptively increases (resp. decreases) α_T to compensate for systematic under (resp. over) coverage frequency.

To construct the prediction set in (2), one must randomly split the observed data stream $\{(X_t, Y_t)\}_{t=1}^{T-1}$ into training and calibration sets, as visualized in Figure 2a. As a result, to implement ACI, one needs to fit a new prediction model once a new sample (X_T, Y_T) is observed. This may be impractical when the training phase is computationally intensive, as happens when fitting a deep neural network model. Also, splitting the data at random breaks the dependency structure across the time horizon, and this may reduce the predictive power when close-by data points are dependent. To address this issue and reduce the computational complexity, we combine ACI with *online sequential split conformal prediction* (OSSCP) [22], which can be conducted online, to form a strong, feasible baseline method. We refer to it as ACI-Online, as it can work with any online learning algorithm while enjoying the long-range coverage guarantee of ACI. This approach is described in more detail in Supplementary Section E.3 and visualized in Figure 2b. We will compare our proposed Rolling CI to this baseline method in the numerical experiments.

3 Proposed Method

3.1 General formulation

We now turn to present Rolling CI—a general framework for uncertainty quantification in an online learning setting, which satisfies the coverage requirement in (1). Suppose we are handed with

a predictive model \mathcal{M}_T , fitted on the entire data stream $\{(X_i, Y_i)\}_{i=1}^{T-1}$ up to time $T-1$, and our goal is to construct a prediction set for future response Y_T given the test feature vector X_T . To do so, we define a function $f(\cdot)$ that gets as an input the test X_T , the fitted model $\mathcal{M}_T \in \mathbb{M}$, and a calibration parameter θ_T , and returns a prediction set

$$\hat{C}_T^{\text{RCI}}(X_T) = f(X_T, \theta_T, \mathcal{M}_T) \in 2^{\mathcal{Y}}. \quad (4)$$

Above, $2^{\mathcal{Y}}$ is the power set of \mathcal{Y} . The prediction set is constructed using the fitted model \mathcal{M}_T (which was trained on all data before time T) and the calibration parameter θ . The model $\mathcal{M}_T(X_T)$ is used to form a prediction for Y_T given the current feature vector X_T . In Sections 3.2 and 3.3 we provide concrete formulations for the function f and in Section 3.2.1 we give a specific example for \mathcal{M} . The calibration parameter $\theta_T \in \mathbb{R}$ controls the size of the prediction set generated by f : larger θ_T leads to larger sets, and smaller θ_T leads to smaller sets. As a consequence, θ_T allows us to control the long-range coverage frequency: by increasing (resp. decreasing) θ_T over time we increase (resp. decrease) the coverage rate. Once Y_T is revealed to us, we tune it, as in **ACI**, according to the following rule:

$$\theta_{T+1} = \theta_T + \gamma(\text{err}_T - \alpha), \quad (5)$$

where $\text{err}_T = \mathbb{1}\{Y_T \notin \hat{C}_T(X_T)\}$ is the miscoverage identifier. Lastly, we obtain a new predictive model \mathcal{M}_{T+1} by updating the older one \mathcal{M}_T with the new pair (X_T, Y_T) , e.g., by applying a single gradient step to reduce any given predictive loss function. For convenience, the **Rolling CI** procedure is illustrated in Figure 2c and summarized in Algorithm 1. The validity of our proposal is

Algorithm 1 Rolling CI

Input:

Data $\{(X_t, Y_t)\}_{t=1}^T \subseteq \mathcal{X} \times \mathcal{Y}$, given as a stream, miscoverage level $\alpha \in (0, 1)$, a step size $\gamma > 0$, an interval/set constructing function $f : (\mathcal{X}, \mathbb{R}, \mathbb{M}) \rightarrow 2^{\mathcal{Y}}$ and an online learning model \mathcal{M} .

Process:

- 1: Initialize $\theta_0 = 0$.
- 2: **for** $t = 1, \dots, T$ **do**
- 3: Construct a prediction set for the new point X_t : $\hat{C}_t^{\text{RCI}}(X_t) = f(X_t, \theta_t, \mathcal{M}_t)$.
- 4: Obtain Y_t .
- 5: Compute $\text{err}_t = \mathbb{1}\{Y_t \notin \hat{C}_t^{\text{RCI}}(X_t)\}$.
- 6: Update $\theta_{t+1} = \theta_t + \gamma(\text{err}_t - \alpha)$.
- 7: Fit the model \mathcal{M}_t on (X_t, Y_t) and obtain the updated model \mathcal{M}_{t+1} .
- 8: **end for**

Output:

Uncertainty sets $\hat{C}_t^{\text{RCI}}(X_t)$ for each time step $t \in \{1, \dots, T\}$.

given below, whose proof is deferred to Supplementary Section A.1.

Theorem 1. Suppose that $f : (\mathcal{X}, \mathcal{R}, \mathbb{M}) \rightarrow 2^{\mathcal{Y}}$ is an interval/set constructing function. In addition, suppose that there exist constants m and M such that for all X and \mathcal{M} , $f(X, \theta, \mathcal{M}) = \emptyset$ for all $\theta < m$ and $f(X, \theta, \mathcal{M}) = \mathcal{Y}$ for all $\theta > M$. Consider the following series of calibrated intervals: $\{\hat{C}_t^{\text{RCI}}(X_t)\}_{t=1}^{\infty}$, where $\hat{C}_t^{\text{RCI}}(X_t)$ is defined according to (4). The calibrated intervals satisfy the coverage requirement in (1).

Crucially, this theorem states that the coverage guarantee of **Rolling CI** holds for any distribution $\{P_{X_t, Y_t}\}_t$, any set-valued function f , and any sequence of online-updated predictive models $\{\mathcal{M}_t\}_t$. The only requirement for Theorem 1 to hold is that the function f must yield the empty set for small enough θ and the full label space for large enough θ . Also, note that the updating rate γ and the bounds m, M must be fixed in order to control the coverage. Any set-valued function can be modified easily to satisfy this property, so this does not limit the scope of our proposed algorithm.

The intuition behind **Rolling CI** and Theorem 1 is the following: we track the past coverage rate and correct the coverage frequency over time by modifying the length of future intervals. If the past coverage rate is too high (e.g. above 90%), we shorten the intervals by decreasing θ , which, in turn, is anticipated to reduce the future coverage rate. If the past coverage rate is too low, we widen the intervals by increasing θ , which, in turn, is anticipated to increase the future coverage rate. We also

note that although we use the same data point twice, our method is immune to over-fitting by design: we first use the new labeled data for calibration, and only then for updating the machine learning model, as stated in steps 6 and 7 of Algorithm 1. That is, the evaluation of θ_t is conducted by using the predictions produced by an “old” model, before updating it with the new labeled point.

We also note that the proof of Theorem 1 gives finite-samples bounds for how close the realized coverage is to the desired level; the empirical coverage falls within a C/T factor of the desired level $1 - \alpha$, where C is a known constant. See Supplementary Section A.1 for details. Furthermore, our new formulation unlocks new design possibilities: we can define any prediction set function f while guaranteeing the validity of its output by calibrating any parameter θ_t . This parameter can affect f in a highly non-linear fashion to attain the most informative (i.e., small) prediction sets. Of course, the performance of the proposed scheme is influenced by the design of f , which is the primary focus of the next sections.

3.2 Rolling CI for Regression

In this section, we introduce two concrete formulations for the function f , by building upon recent advances in conformal prediction for regression problems. The two formulations we present below seek to construct prediction intervals (rather than sets) that are short and highly adaptive.

3.2.1 Calibrating in \mathcal{Y} Scale

Consider a *quantile regression* model \mathcal{M}_t that produces estimates for the $\alpha/2$ and $1 - \alpha/2$ conditional quantiles of the distribution of $Y_t | X_t$ —we denote these as $\mathcal{M}_t(X_t, \alpha/2)$ and $\mathcal{M}_t(X_t, 1 - \alpha/2)$, respectively. Estimating the conditional quantile function can be done, for example, by minimizing the pinball loss in lieu of the standard mean squared error loss used in classic regression; see [24–28]. Specifically, in our experiments we minimize the objective function:

$$\min_{\mathcal{M}_t} \sum_{t'=1}^t \rho_{\alpha/2}(Y_{t'}, \mathcal{M}_t(X_{t'}, \alpha/2)) + \rho_{1-\alpha/2}(Y_{t'}, \mathcal{M}_t(X_{t'}, \alpha/2)),$$

where $\rho_{\alpha}(y, \hat{y}) = \begin{cases} \alpha(y - \hat{y}) & y - \hat{y} > 0, \\ (1 - \alpha)(\hat{y} - y) & \text{otherwise.} \end{cases}$ is the pinball loss. In our experiments, we formulate \mathcal{M}_t as an LSTM model and minimize the above cost function in an online fashion as follows.

Given a new labeled test point (X_t, Y_t) , we (i) compute the pinball loss both for the lower and upper quantiles, i.e., $\rho_{\alpha/2}(Y_t, \mathcal{M}_t(X_t, \alpha/2))$ and $\rho_{1-\alpha/2}(Y_t, \mathcal{M}_t(X_t, 1 - \alpha/2))$, respectively; and (ii) update the parameters of the LSTM model \mathcal{M}_t by applying a few gradient steps with ADAM optimizer. More details on the network architecture are given in Supplementary Section B.1.

The guiding principle here is that a model that perfectly estimates the conditional quantiles for any time step t will form small intervals with the desired $1 - \alpha$ coverage level. In practice, however, the model \mathcal{M}_t estimating the conditional quantiles may not be accurate, and thus may result in a coverage rate lower or higher than the desired one; this is especially true for data with frequent time-varying distributional shifts. Consequently, to ensure valid coverage, we apply Rolling CI. Taking inspiration from the method of conformalized quantile regression (CQR) [29], we use the following interval construction function:

$$f(X_t, \theta_t, \mathcal{M}_t) = [\mathcal{M}_t(X_t, \alpha/2) - \varphi(\theta_t), \mathcal{M}_t(X_t, 1 - \alpha/2) + \varphi(\theta_t)]. \quad (6)$$

Above, the interval endpoints are obtained by augmenting the lower and upper estimates of the conditional quantiles by an additive calibration term $\varphi(\theta_t)$. The role of θ_t is the same as before: the larger θ_t , the wider the resulting interval is. Here, however, we introduce an additional stretching function φ that can scale θ_t non-linearly, providing us the ability to adapt more quickly to severe distributional shifts. We now present two design options for the stretching function φ , and discuss their effect on the resulting intervals.

Linear. The first and perhaps most natural option is $\varphi(x) = x$, which does not stretch the scale of the interval’s adjustment factor. While this is the most simple choice, it might be sub-optimal when an aggressive and fast calibration is required. To see this, recall (5), and observe that the step size γ used to update θ_t must be fixed throughout the entire process. As a result, the calibration parameter θ_t might be updated too slowly, resulting in an unnecessary delay in the interval’s adjustment. To overcome this limitation, we now turn to present the following alternative.

Exponential. The exponential stretching function, defined as $\varphi(x) = e^x - 1$ for $x > 0$ and $\varphi(x) = -e^{-x} + 1$ for $x \leq 0$, updates the calibration adjustment factor with an exponential rate: $\varphi'(x) = e^x$, even though the step size for θ_t is fixed. In other words, it updates $\varphi(\theta_t)$ gently when the calibration is mild ($\varphi(\theta_t)$ is close to 0), and faster as the calibration is more aggressive ($\varphi(\theta_t)$ is away from zero).

This discussion sheds light on the great flexibility of Rolling CI: we can accurately find the correct calibration parameter while being adaptive to rapid distributional shifts in the data.

3.2.2 Calibrating on the Quantile Scale

As an alternative for (6), where the calibration coefficient $\varphi(\theta_t)$ is added to each of the interval endpoints, one can modify the interval's length by tuning the raw miscoverage level $\tau_t = \varphi(\theta_t)$ requested from the model:

$$f(X_t, \theta_t, \mathcal{M}_t) = [\mathcal{M}_t(X_t, \tau_t/2), \mathcal{M}_t(X_t, 1 - \tau_t/2)].$$

This formulation is inspired by the work of [30] that suggested tuning the nominal miscoverage level τ , based on a calibration set. In contrast to (6), where we estimate only the lower $\alpha/2$ and upper $1 - \alpha/2$ conditional quantiles, here, we need to estimate all the quantiles simultaneously. To accomplish this, one can apply the methods proposed in [31–33]. Turning to the choice of the stretching function φ : the straightforward option is to set $\varphi(\theta) = -\tau$, where θ_t is bounded in the range: $-1 \leq \theta_t \leq 0$. The reason for having the negative sign in φ , is to form larger prediction sets (resulted by smaller values of τ) as θ increases.

3.3 Rolling CI for Classification

Consider a multi-class classification problem, where the target variable is discrete and unordered $y \in \mathcal{Y} = \{1, 2, \dots, K\}$. Suppose we are handed with a classifier that estimates the conditional probability of $P_{Y_t|X_t}(Y_t = y | X_t = x)$ for each class y , i.e., $\mathcal{M}_t(X_t, y) \in [0, 1]$ and $\sum_{y \in \mathcal{Y}} \mathcal{M}_t(X_t, y) = 1$. With this in place, we follow [34] and define the prediction set constructing function as:

$$f(X_t, \theta_t, \mathcal{M}_t) = \{y : \mathcal{M}_t(X_t, y) \geq \varphi(\theta_t)\}, \quad (7)$$

where one can choose $\varphi(x) = -x$, for instance. While this procedure is guaranteed to attain the pre-specified coverage level $1 - \alpha$, according to Theorem 1, the function f in (7) may have unbalanced coverage across different sub-populations in the data [35, 36]. To overcome this, we recommend using the function f presented in Section G of the Supplementary Material, which is capable of constructing prediction sets that better adapt to the underlying uncertainty.

3.4 Rolling CI with Calibration Set

We turn to present a specialization of Rolling CI—which we call Rolling CI with cal—that is closer to conformal prediction and ACI. It is more out-of-the-box because it allows the user to take any conformal score function from the conformal prediction literature to get a confidence set function f . Many conformal scores have been developed and extensively studied, so this approach directly inherits all of the progress made on this topic. Rolling CI with cal uses calibration points, but does not hold out a large block like ACI-Online. Rather, previous points are simultaneously used both for calibration and model fitting.

Turning to the details, denote by $S(\mathcal{M}_t(X_t), Y_t) \in \mathbb{R}$ a non-conformity score function that takes as an input the model's prediction $\mathcal{M}_t(X_t)$ at time t and the corresponding label Y_t , and returns a measure for the model's goodness-of-fit or prediction error. Here, the convention is that smaller scores imply a better fit. For instance, adopting the same notations from (6), the quantile regression score presented in [29] are given by $S(\mathcal{M}_t(X_t), Y_t) = \max\{\mathcal{M}_t(X_t, \alpha/2) - Y_t, Y_t - \mathcal{M}_t(X_t, 1 - \alpha/2)\}$. Next, define the prediction set constructing function in (4) as:

$$f(X_t, \theta_t, \mathcal{M}_t) = \{y \in \mathcal{Y} : S(\mathcal{M}_t(X_t), y) \leq Q_{1+\theta_t}(\mathcal{S}_{\text{cal}})\}, \quad (8)$$

where $\mathcal{S}_{\text{cal}} = \{S(\mathcal{M}_{t'}(X_{t'}), Y_{t'}) : t' = t - n, \dots, t - 1\}$ is a set containing the n most recent non-conformity scores. The function $Q_{1+\theta_t}(\mathcal{S}_{\text{cal}})$ returns the $(1 + \theta_t)$ -th empirical quantile of the scores in \mathcal{S}_{cal} , being the $\lceil (1 + \theta_t)(n + 1) \rceil$ largest element in that set. Here, $-1 \leq \theta_t \leq 0$ is the calibration parameter we tune recursively, as in (5). In plain words, f in (8) returns all the candidate

target values y for the test label, whose score $S(\mathcal{M}_t(X_t), y)$ is smaller than $(1 + \theta_t) \times 100\%$ of the scores in S_{cal} , which are evaluated on truly labeled historical data $S(\mathcal{M}_{t'}(X_{t'}), Y_{t'})$. As such, the size of set in (8) gets smaller (larger) as $1 + \theta_t$ gets smaller (larger).

For reference, our Rolling CI with cal procedure is summarized in Algorithm 4 of the Supplementary Material. The reason for this method's name is to emphasize that we now use calibration scores to formulate the prediction set function f . However, we do not reserve a holdout set for calibration as ACI does: our proposed sequential evaluation of the calibration scores is immune to over-fitting by design. It also allows us to work with any online learning algorithm and utilize all the data observed up to time t to train \mathcal{M}_t in an online fashion, as Rolling CI operates. In fact, the coverage guarantee of Rolling CI with cal follows directly from Theorem 1 for $f(X_t, \theta_t, \mathcal{M}_t)$ defined in (8), as stated next.

Corollary 1. *Rolling CI with cal satisfies the coverage guarantee in (1).*

The experiments in Section 5 show that this method indeed performs better than the online version of ACI, but worse than our main proposal, Rolling CI. Perhaps this is due to the indirect approach we take in Rolling CI with cal to adjust the size of the prediction set, which is done only through the calibration scores, as opposed to Rolling CI.

4 Time-Series Conditional Coverage Metrics

In this section, we describe two metrics to assess conditional/local coverage validity in the online learning regime, which we will use in the numerical simulations.

MSL: As implied by its name, the metric *miscoverage streak length* evaluates the average length of miscoverage streaks of the constructed prediction intervals. Formally, given a series of intervals $\{\hat{C}_t(X_t)\}_{t=T_0}^{T_1} \subseteq 2^{\mathcal{Y}}$ and response variables $\{Y_t\}_{t=T_0}^{T_1} \subseteq \mathcal{Y}$, the MSL metric is defined as:

$$\text{MSL} := \frac{1}{|\mathcal{I}|} \sum_{t \in \mathcal{I}} \min\{i : Y_{t+i} \in \hat{C}_{t+i}(X_{t+i}) \text{ or } t = T_1\},$$

where \mathcal{I} is a set containing the starting times of all miscoverage streaks; see formal description in Section F.1. To improve the interpretability of this measure, we show in Supplementary Section F.1 that an ideal model that has access to the true conditional quantiles attains an MSL of $1/(1 - \alpha)$. Therefore, we seek to produce the narrowest intervals having an MSL close to this value.

Δ Coverage: The time-series data sets we use in the experiments in Section 5 include the day of the week as an element in the feature vector. Therefore, we assess the violation of day-stratified coverage [22, 37], as a proxy for conditional coverage. That is, we measure the average deviation of the coverage in each day of the week from the nominal coverage level; see Supplementary Section F.2 for a formal definition. Since a lower value of this metric indicates for a better conditional coverage, we desire to have a minimal Δ Coverage.

5 Experiments

5.1 Classic, Single-Output Quantile Regression

In this section, we analyze the effectiveness of our two proposed calibration schemes, Rolling CI and Rolling CI with cal, on five real-world benchmark data sets: power [38], energy [39], traffic [40] wind [41], and prices [42]. We provide more details about these data sets in Section D.2. The evaluation protocol is as follows. We commence by fitting an initial quantile regression model on the first 5000 data points, to obtain a reasonable predictive system. Then, passing time step 5001, we start applying the calibration procedure while continuing to fit the model in an online fashion; we keep doing so until reaching time step 10000. Lastly, we measure the performance of the deployed calibration method on data points corresponding to time steps 8001 to 10000. In all experiments, we fit an LSTM predictive model [43] in an online fashion, minimizing the pinball loss to estimate the 0.05 and 0.95 conditional quantiles of $Y_t | X_t$; these estimates are used to construct prediction intervals with target 90% coverage rate. For both ACI-Online and Rolling CI with cal, we use the CQR scores [29] to calibrate the prediction intervals with a calibration set of size 300. As for Rolling CI, we calibrate the intervals in y scale with an exponential stretching, as described in

Section 3.2.1. We repeat each experiment for 20 random initializations of the neural network model. Section B of the Supplementary Material provides more details regarding the network architecture, hyper-parameters tuning, training strategy, and the experimental setup.

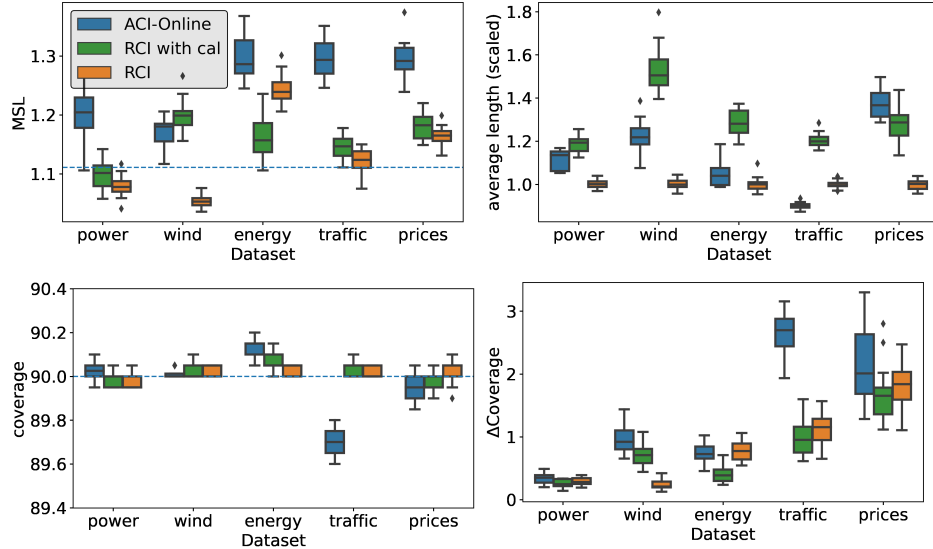


Figure 3: Performance of ACI-Online, Rolling CI with cal, and Rolling CI on real data sets. The length of the prediction intervals are scaled by the average length of the intervals constructed by Rolling CI.

Figure 3 summarizes the performance metrics presented in Section 4, showing that all methods attain the desired coverage level; this is guaranteed by Theorem 1. That figure also shows that our Rolling CI constructs the narrowest intervals while attaining the best conditional coverage metrics. Additionally, one can see that RCI with cal tends to construct intervals of better conditional coverage than ACI-Online, as indicated by the MSL and Δ Coverage metrics. This, however, comes at the cost of widening the intervals' length.

5.2 Multiple-Output Quantile Regression

We now introduce an application of our calibration scheme for which the response is a multivariate vector ($\mathcal{Y} = \mathbb{R}^d$) rather than a one-dimensional scalar. Here, our goal is to construct a predictive *region* (not an interval) in the multivariate space that covers $1 - \alpha$ of the response vectors over long intervals of time, as in (1). In the interest of space, we provide the full experimental description in Section C.3, and here we only present the results of our proposal on one data set: a multivariate-response version of the power data [38], explained in Supplementary Section D.3. The peculiarity of this experiment is that calibration-set-based methods, such as ACI-Online, cannot be deployed in this setting. In Section C.3, we carefully argue why the anticipated total run-time of ACI-Online would be about 8.4 months of GPU computations, while the run-time of Rolling CI is less than half an hour. Therefore, our proposal has a fractional speed up of 12,500 (!), being the only calibration scheme that can be applied in this multivariate-response setting.

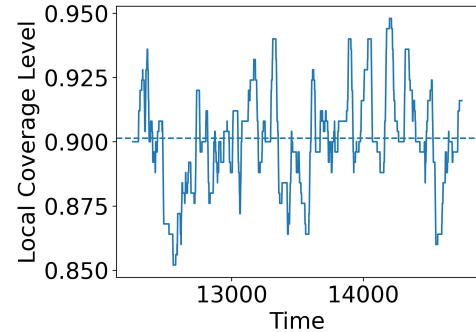


Figure 4: Local coverage rates of predictive regions constructed by our method for the multiple-response version of the power data set.

To evaluate the performance of our method, we assess the coverage validity in local windows in time via the metric of *local coverage frequencies* proposed in [21] and formulated as: $\text{localCov}_t := 1 - 1/500 \sum_{r=t-250+1}^{t+250} \text{err}_r$. The local coverage rates of the predictive regions constructed by Rolling CI for this multivariate-response data are displayed in Figure 4, showing that our technique leads to the desired coverage level, guaranteed by Theorem 1. Importantly, the local coverage is close to the nominal level throughout the entire process, indicating good conditional coverage.

6 Discussion

To conclude, we summarize the properties of our proposal compared to other conformal calibration techniques for adversarial sequences in Table 1. While valid calibration is an important step toward making learning systems safer, fairer, and more robust, we emphasize that calibration is not a panacea and one must always treat data with care—especially when data-driven predictions are used for high-stakes decisions. In particular, the flexibility of our proposed method is a mixed blessing, in that the system builder has the ability and responsibility to make important design choices. These choices can have important consequences, so they must be treated with care. We offer initial guidelines herein, acknowledging that of course, they do not anticipate the consequences in all possible use cases. Nonetheless, we highlight that uncertainty quantification is an important component to designing learning systems to have a positive impact in the real world, where the data are complex and distributions are continually shifting. Our work makes one step toward this goal.

Table 1: A summary of all sequential calibration methods described in this paper.

Calibration method	Is online	Has a coverage guarantee	The model uses all data
ACI [21]	✗	✓	✗
OSSCP [22]	✓	✗	✗
ACI-Online ([21, 22] and Supplementary Section E.3)	✓	✓	✗
Rolling CI with cal	✓	✓	✓
Rolling CI	✓	✓	✓

Acknowledgments and Disclosure of Funding

Y.R. and S.F. were supported by the ISRAEL SCIENCE FOUNDATION (grant No. 729/21). Y.R. also thanks the Career Advancement Fellowship, Technion, for providing research support.

References

- [1] Timothy John Sullivan. *Introduction to uncertainty quantification*, volume 63. Springer, 2015.
- [2] Christian Soize. *Uncertainty quantification*. Springer, 2017.
- [3] Surya Mattu Julia Angwin, Jeff Larson and ProPublica Lauren Kirchner. Machine bias: There’s software used across the country to predict future criminals. and it’s biased against blacks, 2016.
- [4] Francisco Díaz-González, Andreas Sumper, Oriol Gomis-Bellmunt, and Roberto Villafáfila-Robles. A review of energy storage technologies for wind power applications. *Renewable and sustainable energy reviews*, 16(4):2154–2171, 2012.
- [5] Jaquelin Cochran, Paul Denholm, Bethany Speer, and Mackay Miller. Grid integration and the carrying capacity of the us grid to incorporate variable renewable energy. Technical report, National Renewable Energy Lab.(NREL), Golden, CO (United States), 2015.
- [6] Lewis H. Mervin, Simon Johansson, Elizaveta Semenova, Kathryn A. Giblin, and Ola Engkvist. Uncertainty quantification in drug design. *Drug Discovery Today*, 26(2):474–489, 2021.
- [7] Ryutaro Tanno, Daniel E. Worrall, Enrico Kaden, Aurobrata Ghosh, Francesco Grussu, Alberto Bazzi, Stamatios N. Sotiropoulos, Antonio Criminisi, and Daniel C. Alexander. Uncertainty modelling in deep learning for safer neuroimage enhancement: Demonstration in diffusion MRI. *NeuroImage*, 225:117366, 2021.

- [8] Edmon Begoli, Tanmoy Bhattacharya, and Dimitri F. Kusnezov. The need for uncertainty quantification in machine-assisted medical decision making. *Nature Machine Intelligence (Online)*, 1(1), 1 2019.
- [9] Varun Babbar, Umang Bhatt, and Adrian Weller. On the utility of prediction sets in human-AI teams. *arXiv preprint arXiv:2205.01411*, 2022.
- [10] Vladimir Vovk, Alex Gammerman, and Glenn Shafer. *Algorithmic Learning in a Random World*. Springer, 2005.
- [11] Stephen Bates, Anastasios Angelopoulos, Lihua Lei, Jitendra Malik, and Michael I. Jordan. Distribution-free, risk-controlling prediction sets. *Journal of the ACM*, 68(6), September 2021.
- [12] Anastasios Nikolas Angelopoulos and Stephen Bates. A gentle introduction to conformal prediction and distribution-free uncertainty quantification. *arXiv preprint*, 2021. arXiv:2107.07511.
- [13] Glenn Shafer and Vladimir Vovk. A tutorial on conformal prediction. *Journal of Machine Learning Research*, 9(3), 2008.
- [14] Emmanuel J Candès, Lihua Lei, and Zhimei Ren. Conformalized survival analysis. *arXiv preprint arXiv:2103.09763*, 2021.
- [15] Chen Xu and Yao Xie. Conformal prediction interval for dynamic time-series. In Marina Meila and Tong Zhang, editors, *Proceedings of the 38th International Conference on Machine Learning*, volume 139 of *Proceedings of Machine Learning Research*, pages 11559–11569. PMLR, 18–24 Jul 2021.
- [16] Chen Xu and Yao Xie. Conformal prediction interval for dynamic time-series. In Marina Meila and Tong Zhang, editors, *Proceedings of the 38th International Conference on Machine Learning*, volume 139 of *Proceedings of Machine Learning Research*, pages 11559–11569. PMLR, 18–24 Jul 2021.
- [17] Victor Chernozhukov, Kaspar Wüthrich, and Zhu Yinchu. Exact and robust conformal inference methods for predictive machine learning with dependent data. In *Conference On Learning Theory*, pages 732–749. PMLR, 2018.
- [18] Maxime Cauchois, Suyash Gupta, Alnur Ali, and John C Duchi. Robust validation: Confident predictions even when distributions shift. *arXiv preprint arXiv:2008.04267*, 2020.
- [19] Ryan J Tibshirani, Rina Foygel Barber, Emmanuel Candes, and Aaditya Ramdas. Conformal prediction under covariate shift. *Advances in neural information processing systems*, 32, 2019.
- [20] Kamile Stankeviciute, Ahmed M Alaa, and Mihaela van der Schaar. Conformal time-series forecasting. *Advances in Neural Information Processing Systems*, 34, 2021.
- [21] Isaac Gibbs and Emmanuel Candes. Adaptive conformal inference under distribution shift. In A. Beygelzimer, Y. Dauphin, P. Liang, and J. Wortman Vaughan, editors, *Advances in Neural Information Processing Systems*, 2021.
- [22] Margaux Zaffran, Olivier Féron, Yannig Goude, Julie Josse, and Aymeric Dieuleveut. Adaptive conformal predictions for time series. In *International Conference on Machine Learning*, pages 25834–25866. PMLR, 2022.
- [23] Jing Lei, Max G’Sell, Alessandro Rinaldo, Ryan J Tibshirani, and Larry Wasserman. Distribution-free predictive inference for regression. *Journal of the American Statistical Association*, 113(523):1094–1111, 2018.
- [24] Roger Koenker and Gilbert Bassett. Regression quantiles. *Econometrica*, 46(1):33–50, 1978.
- [25] Rafael Izbicki, Gilson Shimizu, and Rafael Stern. Flexible distribution-free conditional predictive bands using density estimators. In *Proceedings of the Twenty Third International Conference on Artificial Intelligence and Statistics*, volume 108, pages 3068–3077. PMLR, 26–28 Aug 2020.

[26] Nicolai Meinshausen. Quantile regression forests. *J. Mach. Learn. Res.*, 7:983–999, December 2006.

[27] Yichen Jia and Jong-Hyeon Jeong. Deep learning for quantile regression under right censoring: DeepQuantreg. *Comput. Stat. Data Anal.*, 165(C), jan 2022.

[28] Roger Koenker and Kevin F. Hallock. Quantile regression. *Journal of Economic Perspectives*, 15(4):143–156, December 2001.

[29] Yaniv Romano, Evan Patterson, and Emmanuel Candes. Conformalized quantile regression. In *Advances in Neural Information Processing Systems*, volume 32, 2019.

[30] Victor Chernozhukov, Kaspar Wüthrich, and Yinchu Zhu. Distributional conformal prediction. *Proceedings of the National Academy of Sciences*, 118(48), 2021.

[31] Youngsuk Park, Danielle Maddix Robinson, Yuyang (Bernie) Wang, and Jan Gasthaus. Learning quantile function without quantile crossing for distribution-free time series forecasting. In *ICML 2021 Workshop on Distribution-Free Uncertainty Quantification*, 2021.

[32] Youngseog Chung, Willie Neiswanger, Ian Char, and Jeff Schneider. Beyond pinball loss: Quantile methods for calibrated uncertainty quantification. In A. Beygelzimer, Y. Dauphin, P. Liang, and J. Wortman Vaughan, editors, *Advances in Neural Information Processing Systems*, 2021.

[33] Matteo Sesia and Yaniv Romano. Conformal prediction using conditional histograms. In A. Beygelzimer, Y. Dauphin, P. Liang, and J. Wortman Vaughan, editors, *Advances in Neural Information Processing Systems*, 2021.

[34] Harris Papadopoulos, Kostas Proedrou, Volodya Vovk, and Alex Gammerman. Inductive confidence machines for regression. In Tapio Elomaa, Heikki Mannila, and Hannu Toivonen, editors, *Machine Learning: ECML 2002*, pages 345–356, Berlin, Heidelberg, 2002. Springer Berlin Heidelberg.

[35] Maxime Cauchois, Suyash Gupta, and John C. Duchi. Knowing what you know: valid and validated confidence sets in multiclass and multilabel prediction. *Journal of Machine Learning Research*, 22(81):1–42, 2021.

[36] Anastasios Angelopoulos, Stephen Bates, Jitendra Malik, and Michael I. Jordan. Uncertainty sets for image classifiers using conformal prediction. *arXiv preprint*, 2020. arXiv:2009.14193.

[37] Shai Feldman, Stephen Bates, and Yaniv Romano. Improving conditional coverage via orthogonal quantile regression. *arXiv preprint arXiv:2106.00394*, 2021.

[38] Power consumption of tetouan city. <https://archive.ics.uci.edu/ml/datasets/Power+consumption+of+Tetouan+city>. Accessed: April, 2021.

[39] Appliances energy prediction. <https://archive.ics.uci.edu/ml/datasets/Appliances+energy+prediction>. Accessed: April, 2021.

[40] Metro interstate traffic volume. <https://archive.ics.uci.edu/ml/datasets/Metro+Interstate+Traffic+Volume>. Accessed: April, 2021.

[41] Wind power in germany. <https://www.kaggle.com/datasets/1311ff/wind-power>. Accessed: April, 2021.

[42] French electricity spot prices. https://github.com/mzaffran/AdaptiveConformalPredictionsTimeSeries/blob/main/data_prices/Prices_2016_2019_extract.csv. Accessed: April, 2021.

[43] Sepp Hochreiter and Jürgen Schmidhuber. Long short-term memory. *Neural computation*, 9:1735–80, 12 1997.

[44] Diederik P. Kingma and Jimmy Ba. Adam: A method for stochastic optimization. In *3rd International Conference on Learning Representations*, 2015.

- [45] Kihyuk Sohn, Honglak Lee, and Xinchen Yan. Learning structured output representation using deep conditional generative models. *Advances in Neural Information Processing Systems*, 28:3483–3491, 2015.
- [46] S. Kullback and R. A. Leibler. On Information and Sufficiency. *The Annals of Mathematical Statistics*, 22(1):79 – 86, 1951.
- [47] Solomon Kullback. *Information Theory and Statistics*. Courier Corporation, 1997.
- [48] Shai Feldman, Stephen Bates, and Yaniv Romano. Calibrated multiple-output quantile regression with representation learning. *arXiv preprint arXiv:2110.00816*, 2021.
- [49] Jing Lei and Larry Wasserman. Distribution-free prediction bands for non-parametric regression. *Journal of the Royal Statistical Society: Series B (Statistical Methodology)*, 76(1):71–96, 2014.
- [50] Yaniv Romano, Matteo Sesia, and Emmanuel Candès. Classification with valid and adaptive coverage. In *Advances in Neural Information Processing Systems*, volume 33, pages 3581–3591, 2020.
- [51] Victor Chernozhukov, Kaspar Wüthrich, and Yinchu Zhu. Distributional conformal prediction. *Proceedings of the National Academy of Sciences*, 118(48):e2107794118, 2021.
- [52] Peter Hoff. Bayes-optimal prediction with frequentist coverage control. *arXiv preprint arXiv:2105.14045*, 2021.
- [53] Harris Papadopoulos, Alex Gammerman, and Volodya Vovk. Normalized nonconformity measures for regression conformal prediction. In *Proceedings of the IASTED International Conference on Artificial Intelligence and Applications (AIA 2008)*, pages 64–69, 2008.
- [54] Harris Papadopoulos, Vladimir Vovk, and Alexander Gammerman. Regression conformal prediction with nearest neighbours. *Journal of Artificial Intelligence Research*, 40:815–840, 2011.
- [55] Ulf Johansson, Henrik Boström, Tuve Löfström, and Henrik Linusson. Regression conformal prediction with random forests. *Machine learning*, 97(1):155–176, 2014.
- [56] Anastasios N. Angelopoulos, Stephen Bates, Emmanuel J. Candès, Michael I. Jordan, and Lihua Lei. Learn then test: Calibrating predictive algorithms to achieve risk control. *arXiv preprint*, 2021. arXiv:2110.01052.

Appendices

A Theoretical Results

A.1 Proof of Theorem 1

The proof of Theorem 1 is based on that of Proposition 4.1 in [21]. While the proof is similar, our work greatly enlarges the scope of the result.

Proof. Since $f(X, \theta, \mathcal{M}) = \mathcal{Y}$ for $\theta > M$ and $f(X, \theta, \mathcal{M}) = \emptyset$ for $\theta < m$, we get that $\theta \in [m - \gamma, M + \gamma]$. Denote $m' = m - \gamma$, and $M' = M + \gamma$. We follow the proof of [21, Proposition 4.1] and expand the recursion defined in (5):

$$[m', M'] \ni \theta_{T+1} = \theta_1 + \sum_{t=1}^T \gamma(\text{err}_t - \alpha).$$

By rearranging this we get that:

$$\frac{m' - \theta_1}{T\gamma} \leq \frac{1}{T} \sum_{t=1}^T (\text{err}_t - \alpha) = \frac{\theta_{T+1} - \theta_1}{T\gamma} \leq \frac{M' - \theta_1}{T\gamma}.$$

Therefore:

$$\left| \frac{1}{T} \sum_{t=1}^T (\text{err}_t - \alpha) \right| \leq \frac{\max \{\theta_1 - m', M' - \theta_1\}}{T\gamma}.$$

Lastly, the definition of the miscoverage event, $\text{err}_t = \mathbb{1}_{\{Y_t \notin \hat{C}_t(X_t)\}}$, gives us the coverage statement in (1). \square

Notice that the above proof additionally implies a finite-sample bound for the deviation of the empirical miscoverage rate from the desired level. In particular, the average miscoverage is within a C/T factor of α , where $C = (M' - m')/\gamma = (M - m + 2\gamma)/\gamma$. This bound is deterministic, not probabilistic. Thus, even for the most erratic input sequences, the method has average coverage very close to the nominal level.

B Experimental Setup

B.1 Single-Output Setup

The neural network architecture is composed of four parts: an MLP, an LSTM, and another two MLPs. To estimate the uncertainty of $Y_t | X_t$, we first map the previous k samples $\{(X_{t-i}, Y_{t-i}, \tau)\}_{i=1}^k$ through the first MLP, denoted as f_1 ,

$$w_{t-i}^1 = f_1(x_{t-i}, y_{t-i}, \tau),$$

where we set k to 3 in our experiments. The outputs are then forwarded through the LSTM network, denoted as f_2 :

$$\{w_{t-i}^2\}_{i=1}^k = f_2(\{w_{t-i}^1\}_{i=1}^k).$$

Note that since f_2 is an LSTM model, w_{t-i}^2 is used to compute w_{t-i+1}^2 . The last output w_{t-1}^2 of the LSTM model, being an aggregation of the previous k samples, is fed, together with (X_t, τ) , to the second MLP model, denoted as f_3 :

$$w_t^3 = f_3(w_{t-1}^2, X_t).$$

Lastly, we pass w_t^3 through the third MLP, denoted by f_4 , with one hidden layer that contains 32 neurons:

$$\mathcal{M}_\tau(X_t) = f_4(w_t^3, \tau).$$

The networks contain dropout layers with a parameter equal to 0.1. The model's optimizer is Adam [44] and the batch size is 512, i.e., the model is fitted on the most recent 512 samples in each time

step. Before forwarding the input to the model, the feature vectors and response variables were normalized to have unit variance and zero mean using the first 8000 samples of the data stream.

Lastly, the exponential stretching function used by `Rolling CI` in the single-output experiment in Section 5.1 is defined as:

$$\varphi(x) = \begin{cases} e^x - 1, & x > 0.1, \\ x, & -0.1 \leq x \leq 0.1, \\ -e^{-x} + 1, & x < -0.1, \end{cases}$$

B.2 Multiple-Output Quantile Regression Experimental Setup

The STDQR model is composed of a conditional variational auto encoder (CVAE) [45] network that contains an encoder and decoder. We follow the networks notations from Section B.1, and define the initial region constructed by the base model as:

$$\begin{aligned} w_t^3 &= f_3(w_{t-1}^2, X_t), \\ z_t &= \mathcal{E}(w_t^3, X_t, Y_t), \\ \hat{R}_{1-\alpha}(X_t) &= \left\{ \mathcal{D}(z, w_t^3, X_t) : z \in \mathbb{R}^m, \|z\|_2 \leq \sqrt{Q_{\chi_m^2}(1-\alpha)} \right\}, \\ a_0 &= \mathcal{D}(0^r, w_t^3, X_t), \end{aligned}$$

where \mathcal{E} , \mathcal{D} are the encoder and decoder networks of the STDQR model, m is the dimension of z , $Q_{\chi_m^2}$ is the inverse cumulative distribution function (ICDF) of the chi-squared distribution with m degrees of freedom, and 0^r is a vectors of zeros of size r . We fit the model with a batch size of 64 with a loss that penalizes deviation of the output of the encoder \mathcal{E} from the multivariate normal distribution using the KL-divergence loss [46, 47]. We also added a mean squared error loss to encourage the decoder's \mathcal{D} output to faithfully reconstruct Y , as explained in [48]. The model's hyper-parameters are summarized in Table 2. Since the size of the quantile region $\hat{R}_{1-\alpha}(X_t)$ is continuous (it is a mapping of all $z \in \mathbb{R}^m$ through \mathcal{D}), in practice, we estimated it using 5000 values of z that were sampled from the standard normal distribution. We say that a point $y \in \mathcal{Y}$ is inside the quantile region $\hat{R}_{1-\alpha}(X_t)$ according to the following rule:

$$\begin{aligned} D_t &= \left\{ \min_{u \in (\hat{R}_{1-\alpha}(X_t) - \{a_i\})} d(a_i, u) : a_i \in \hat{R}_{1-\alpha}(X_t) \right\} \\ y \in \hat{R}_{1-\alpha}(X_t) &\iff \min_{u \in \hat{R}_{1-\alpha}(X_t)} d(y, u) \leq q_{0.8}(D_t). \end{aligned}$$

Above, d is Euclidean distance, and $q_{0.8}(D_t)$ is the 0.8 empirical quantile of the set D_t . Therefore, checking whether a variable $y \in \mathcal{Y}$ belongs to $\hat{R}_{1-\alpha}(X_t)$ requires iterating over all 5000 points in the quantile region. We turn this process more efficient by evaluating it over batches, by taking a batch of points in $\hat{R}_{1-\alpha}(X_t)$ and checking their distance from the given target y .

Table 2: Hyperparameters used by the STDQR model

Parameter	Options
f_1 - LSTM input layers	[32, 64, 128]
f_2 - LSTM layers	[64]
f_3 - LSTM output layers	[64]
\mathcal{E} - Encoder layers	[32, 64, 128, 64]
\mathcal{D} - Decoder layers	[32, 64, 128, 64]
learning rate	10^{-3}
drop-out rate	0.1

B.3 Model’s Hyperparameters Tuning

For both real and synthetic data sets we examined all combinations of hyperparameters on one initialization of the model, and manually chose the setting in which the raw model attained the best performance, in terms of coverage and average length. In Section C.1 we present the performance of the methods where the hyperparameters are automatically chosen using a validation set. The combinations we tested are presented in Table 3. Some of the configurations required more than 11GB of memory to train the model, so we did not consider them in our experiments. The updating rates we tested are: $\gamma \in \{0.01, 0.025, 0.05, 0.1, 0.15, 0.2, 0.35\}$. For **ACI**–**Online** we chose the γ that attained the shortest intervals among those who satisfied $\text{MSL} \leq 1.35$. For other calibration techniques, γ was chosen according to Figure 6.

B.4 The Calibration’s Hyperparameters

B.4.1 The Bounds m, M

the lower and upper bounds— m and M are predefined constants serve as safeguards against extreme situations where the data change adversarially over time. In such extreme cases, these bounds allow controlling the coverage: once θ exceeds the upper bound we return the infinite interval (the full label space) and once it exceeds the lower bound we return the empty set. In practice, however, we do not expect a reasonable predictive model to reach the safeguard induced by m and M . In fact, in our experiments, we set $m = -999$, and $M = 999$ to be extremely large values relative to the scale of Y , and the coverage obtained is exactly 90

For classification problems, we can set the bounds to be $(0, 1)$, similarly to **ACI**. For regression problems, it depends on the interval constructing function f . If the intervals are constructed in the quantile scale, according to Section 3.2.2 of the main text, we can set the bounds to be $(0, 1)$ since θ is bounded in this range, as in **ACI**. If the intervals are constructed in the Y scale, according to Section 3.2.1 of the main text, we can set them to be 100 times the difference between the lowest and highest values of the response variables in the training data.

B.4.2 The Initial Value of θ

The recommended way to set the initial value of θ depends on the design of the interval constructing function f : for example, for the interval constructing function in Y scale, presented in Section 3.2.1 in the main text, we set the initial θ to zero as this is the right choice for a model that correctly estimates the conditional quantiles. If the model is inaccurate, θ will be updated over time, in a way that guarantees that the desired long-range coverage will be achieved.

B.4.3 The Learning Rate γ

In this section we analyze the effect of the learning rate γ on the performance of the calibration scheme. Figure 5 presents the results of our **Rolling CI** with a linear stretching function applied with different step-size γ on the synthetic data described in Section 1.1 of the main manuscript. We choose the linear stretching instead of the exponential one to better isolate the effect of γ on the performance. Following that figure, observe that by increasing γ we increase the adaptivity of the method to changes in the distribution of the data, as indicated by the **MSL**. Recall that (i) the lower the **MSL** the smaller the average streak of miscoverage events; and (ii) the **MSL** for the ideal model is ≈ 1.11 . On the other hand, the improvement in **MSL** comes at the cost of increasing the intervals’ lengths: observe how the largest γ results in too conservative intervals, as their **MSL** is equal to 1.

To set a proper value for γ in regression problems, we suggest evaluating the pinball loss of the calibrated intervals, using a validation set. With this approach, one can choose the value of γ that yields the smallest loss. We note that our method is guaranteed to attain valid coverage for any choice of γ , so the trade-off here is between the intervals’ lengths and faster adaptivity to distributional shifts.

B.5 Machine’s Spec

The resources used for the experiments are:

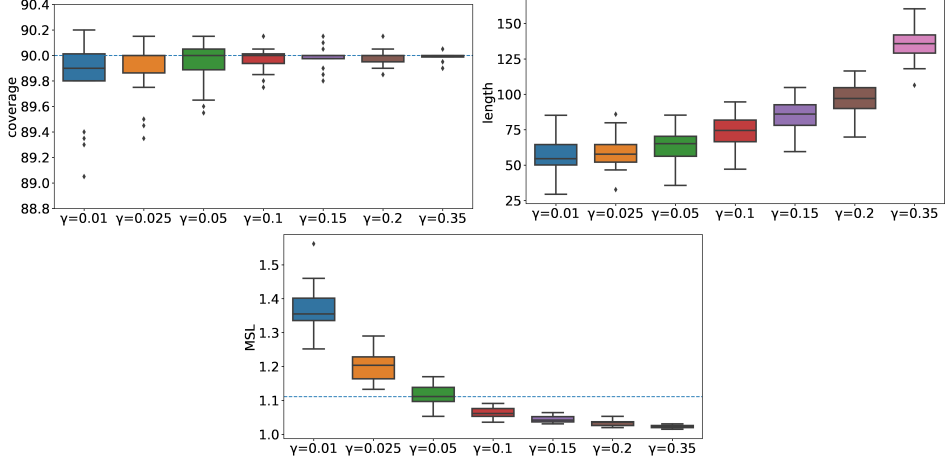


Figure 5: Rolling CI with linear stretching applied with different learning rates on the synthetic described in Section 1.1 of the main manuscript.

- **CPU:** Intel(R) Xeon(R) E5-2650 v4.
- **GPU:** Nvidia titanx, 1080ti, 2080ti.
- **OS:** Ubuntu 18.04.

Table 3: Hyperparameters tested for each data set

Parameter	Options
f_1 - LSTM input layers	[32], [32, 64], [32, 64, 128]
f_2 -LSTM layers	[64], [128]
f_3 -LSTM output layers	[32], [64, 32]
learning rate	10^{-4} , $5 \cdot 10^{-4}$

C Additional Experiments

C.1 Single-Output Quantile Regression - Choosing the Hyperparameters Using a Validation Set

In the following experiment, we select the model’s hyper-parameters, along with the calibration’s learning rate γ , using a validation set, which is independent of the test set. The validation points appear before the test points, indexed from 6000 to 7999, where the test points are indexed by 8001 to 10000. All the performance metrics are evaluated only on the test set. Furthermore, instead of using the scheme provided in Section B.3 for choosing the hyper-parameters, in our revised experiments, the best hyper-parameter configuration was set to be the one achieving the lowest pinball loss on the validation set. The hyper-parameter combinations of the LSTM model we tested are presented in Table 3. The updating rates we tested are: $\gamma \in \{0.05, 0.1, 0.15, 0.2, 0.35\}$. Figure 7 summarizes the results of this experiment, showing that our Rolling CI outperforms the baseline—ACI—Online in terms of both statistical efficiency, as indicated by the average length and conditional coverage, indicated by the MSL and Δ Coverage.

C.2 Single-Output Quantile Regression

In this section, we evaluate Rolling CI in the regression setting for different stretching functions. We follow the procedure described in Section 3.2.1 and use the following stretching functions:

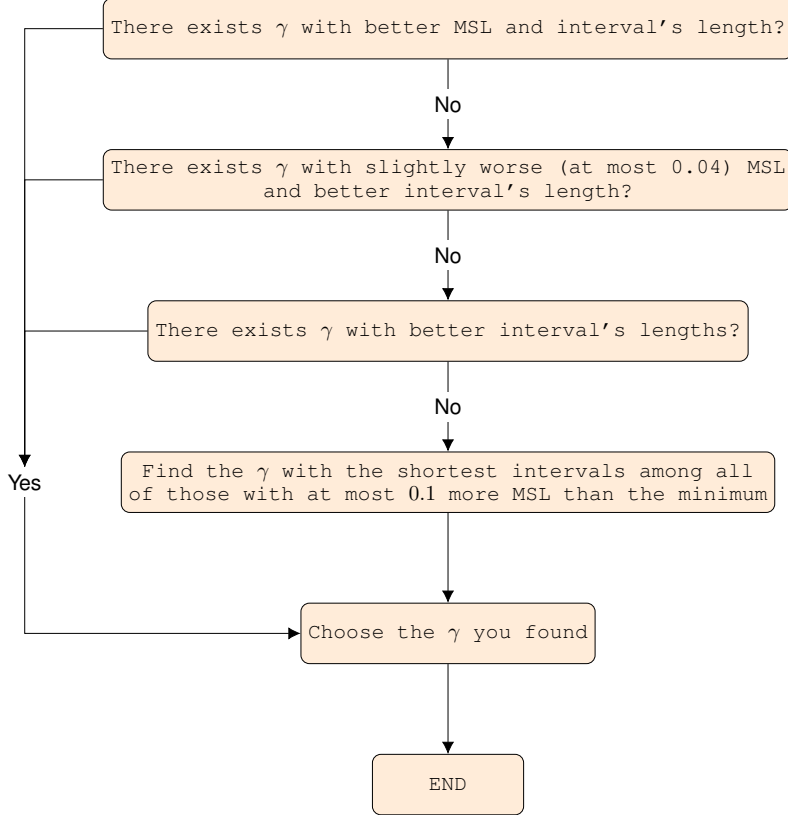


Figure 6: Diagram describing how γ was chosen in our experiments for Rolling CI and Rolling CI with cal calibration schemes.

Linear.

$$\varphi^{\text{linear}}(x) = x$$

Polynomial.

$$\varphi^{\text{poly.}}(x) = \begin{cases} 4x^3, & x > 0.1, \\ x, & -0.1 \leq x \leq 0.1, \\ 4x^3, & x < -0.1, \end{cases}$$

Exponential. We define an exponential stretching given a base $b \in \mathbb{R}$:

$$\varphi_b^{\text{exp.}}(x) = \begin{cases} b^x - 1, & x > 0.1, \\ x, & -0.1 \leq x \leq 0.1, \\ -b^{-x} + 1, & x < -0.1, \end{cases}$$

Notice that all stretching functions are defined as the identity map for $x \in [-0.1, 0.1]$. The reason for this is to apply a slow, linear updating rate when the adjustment factor $\varphi(\theta_t)$ is small, and the intervals require a mild calibration.

Figure 8 displays the performance of Rolling CI with the stretching functions described above. This figure shows that Rolling CI with each stretching function performs well on most of the metrics on most of the data sets.

C.3 Multiple-Output Quantile Regression

We train in an online manner a multiple-output quantile regression model to produce initial quantile regions $\hat{R}_{1-\alpha}(x) \subseteq \mathbb{R}^d$ and then calibrate them with Rolling CI by inflating or shrinking the

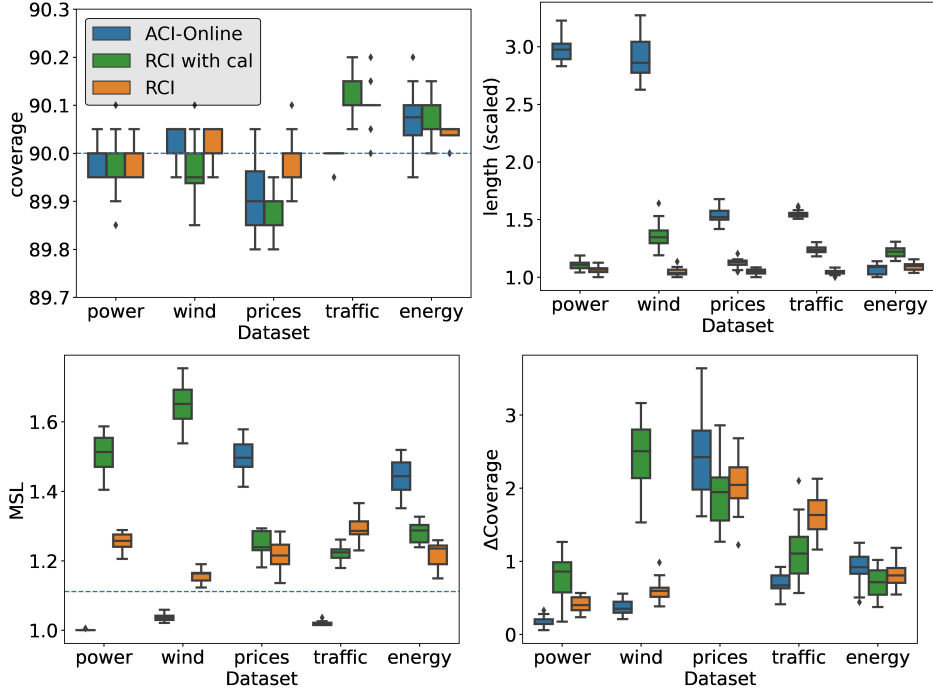


Figure 7: Performance of ACI-Online, Rolling CI with cal, and Rolling CI on real data sets. The length of the prediction intervals are scaled by the minimal length achieved by all methods. The model’s hyper-parameters along with the calibration’s learning rate γ were chosen to minimize the pinball loss over the validation set.

initial region as follows:

$$f(X_t, r_t, \mathcal{M}_t) = \{r_t \cdot (a - a_0) + a_0 : a \in \hat{R}_{1-\alpha}(X_t)\},$$

where a_0 is the center of the region and $r_t = \varphi(\theta_t)$ is the strength of the region adjustment; it expands the initial prediction region for $r_t > 1$, and shrinks it for $r_t < 1$.

We follow the experimental protocol described in Section 5.1, except for training an STDQR [48] as a base model, and using the first 12000 samples of the data stream for normalization and the next 3000 for evaluating performance. Additionally, we start applying our calibration scheme at time step 10000, when the raw model is stabilized. We examine the results on only one data set—a multivariate-response version of the power data [38], see Section D.3 for more details. Also, in this experiment we set the updating rate of θ_t to $\gamma = 0.1$. We provide more details about this experimental setup, including the construction of the initial regions $\hat{R}_{1-\alpha}(x)$ and the definition of the center of the region, a_0 , in Section B.2. The results of this experiment are described in Section 5.2.

We argue that both ACI-Online and Rolling CI with cal cannot tune the parameter r_t throughout the online process. First, as explained in Section B.2, we cannot check the coverage of a set of points in batches, since determining the coverage of only one point is already conducted in batches. Therefore, measuring the coverage rate over the calibration set must be conducted sequentially, iterating over the calibration points one by one, which takes about 0.1 seconds per calibration sample. Second, tuning r_t requires finding the correct inflating strength r_t^* that leads to $1 - \alpha_t$ coverage on the calibration set, every time step. To accomplish this, one must invoke the model every time step with a grid of n_r different values of inflating strengths, and choose the one that attains coverage the closest to the nominal $1 - \alpha_t$ level on the calibration set. Suppose there are $T = 15000$ time steps, $n_{\text{cal}} = 300$ calibration samples, and $n_r = 50$ points in the grid. To conclude, whenever a new sample is revealed, we must compute the coverage over each point in the $n_{\text{cal}} = 300$ calibration set points with n_r different values of $r_t = 50$, which takes $d = 0.1$ seconds per sample. Gathering it all up for $T = 15000$ iterations, the total time duration of the entire process is:

$$T \times n_r \times n_{\text{cal}} \times d = 15000 \times 50 \times 300 \times 0.1 \approx 8.4 \text{ months.}$$

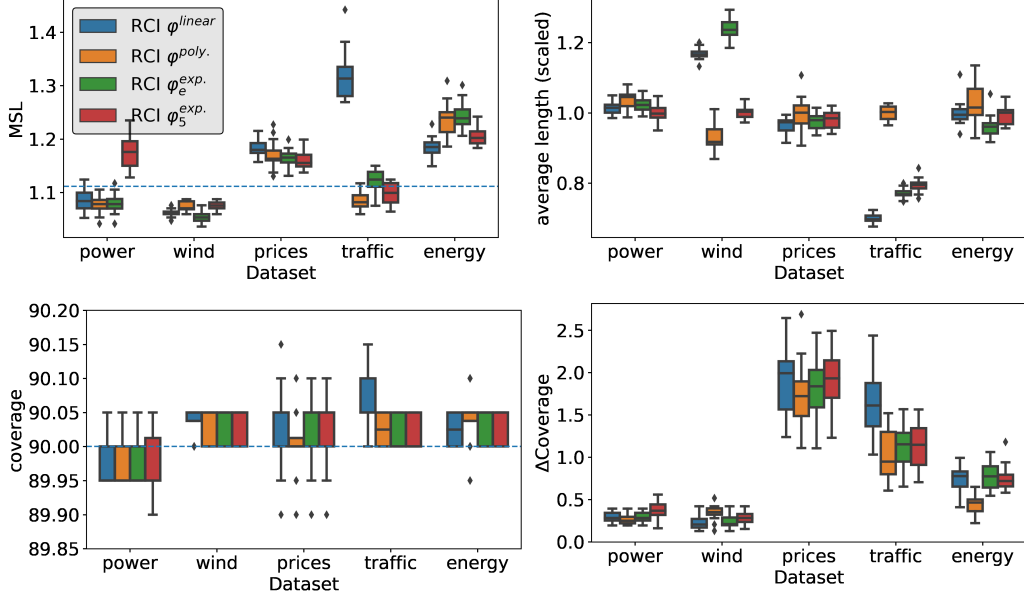


Figure 8: Results of Rolling CI on the real data sets with different stretching functions: identity map (blue), polynomial stretching (orange), exponential stretching with base e (green), and exponential stretching with base 5 (red). For each data set, the intervals’ lengths are scaled by the smallest average length attained among all methods.

Therefore, it is impractical to apply ACI-Online nor Rolling CI with `cal` in this problem.

C.4 Ablation Study on the Time Lag

In this section we provide an experiment that compares two versions of Rolling CI: (i) a sample efficient version of Rolling CI as presented in the paper, implemented without time lag; and (ii) a sample **inefficient** version, implemented with a time lag of length 300 (similarly to ACI-Online). The lagged version of Rolling CI works as follows. Once we are given a test feature vector X_t we construct a prediction interval for the unknown response Y_t using a model \mathcal{M}_t fitted to the samples indexed by $1, 2, \dots, t-300$. Then, we compute the error err_t , using Y_t , and update θ_t according to Equation (5). Next, we update the model \mathcal{M}_t with the sample (X_{t-300}, Y_{t-300}) , by taking a gradient step to reduce the pinball loss. We continue with this process iteratively by fetching a new test sample. The stretching function φ we used is the exponential stretching described in Section 3.2.1. Importantly, we do not recommend using the sample inefficient method (implemented with a time lag), as the model is not fitted to the whole data stream. Yet, this experiment demonstrates the importance of training the model on the most recent points, being one of the key advantages of Rolling CI.

The results are given in Figure 9. This figure shows that the sample efficient version of Rolling CI (i.e., the one implemented without a time lag, which is the method presented in the paper) has superior statistical efficiency compared to the sample inefficient version. This is reflected by the average length, as well as the MSL which is mostly better for the version without the time lag.

D Data Sets Details

D.1 Synthetic Data Set

First, we define a group indication vector, denoted as g_t :

$$g = 1^{m_1} \cdot 2^{m_2} \cdot 3^{m_3} \cdot 4^{m_4} \dots$$

where w^n is a vector of the number w repeated n times, \cdot is a concatenation of two vectors, $m_i \sim \mathcal{N}(500, 10^2)$ and $\mathcal{N}(\mu, \sigma^2)$ is the normal distribution with mean μ and variance σ^2 . In words, each

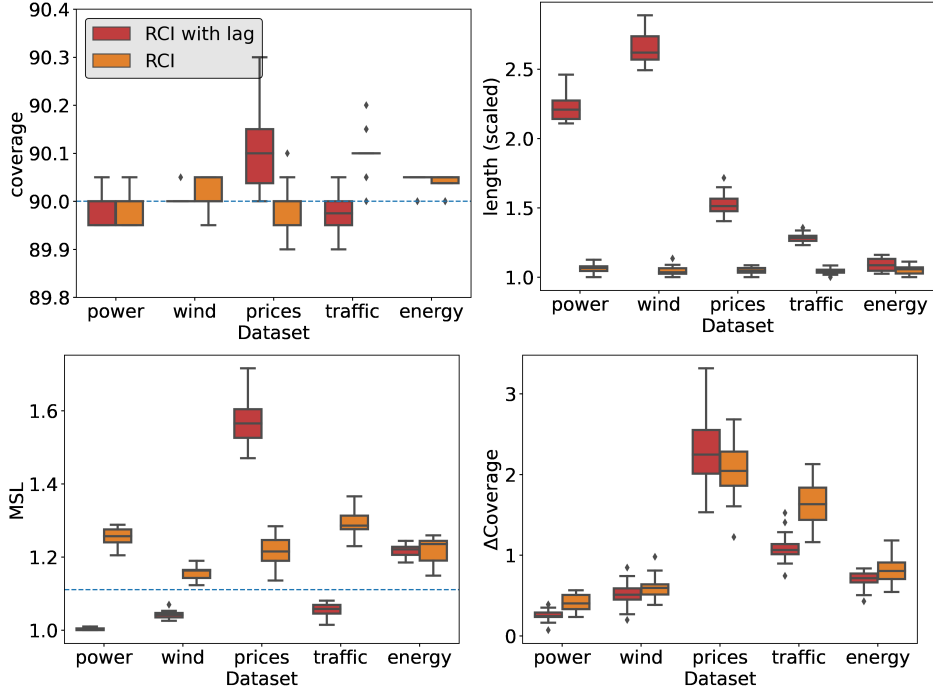


Figure 9: Performance of Rolling CI, as presented in the paper and Rolling CI with time lag of size 300 on real data sets. The length of the prediction intervals are scaled by the minimal length achieved by all methods.

group lasts for approximately 500 time steps, and the vector is a concatenation of the group's indexes. The generation of the feature vectors and the response variable is done in the following way:

$$\begin{aligned}
 \hat{\beta}_i &\sim \text{Uniform}(0, 1)^p, \\
 \beta_i &= \frac{\hat{\beta}_i}{\|\hat{\beta}_i\|_1}, \\
 \omega_i &= \begin{cases} \mathcal{N}(20, 10), & g_t \equiv 0 \pmod{2}, \\ 1, & \text{otherwise,} \end{cases} \\
 X_t &\sim \text{Uniform}(0, 1)^5, \\
 \varepsilon_t &\sim \mathcal{N}(0, 1), \\
 Y_t &= \frac{1}{2} Y_{t-1} + \omega_{g_t}^2 |\beta_{g_t}^T X_t| + 2 \sin(2X_{t,1} \cdot \varepsilon_t),
 \end{aligned}$$

where $\text{Uniform}(a, b)$ is a uniform distribution on the interval (a, b) .

D.2 Real Data Sets

In addition to the features given in the raw data set, we added for each sample the day, month, year, hours, minutes, and the day of the week. Table 4 presents the number of samples in each data set, the number of samples we used in the quantile regression experiments 5.1, and the dimension of the feature vector.

D.3 Multiple-Output Quantile Regression Data Set

In the multiple-output quantile regression experiment in Section 5.2 we evaluated Rolling CI over the power data set [38] that originally contained a one-dimensional target variable. We increased the response dimension by considering the first and second features as response variables instead. These

Table 4: Information about the real data sets.

Data Set	Total Number of Samples	Number of Used Samples	Feature Dimension
power [38]	52416	10000	11
energy [39]	19735	10000	33
traffic [40]	48204	10000	12
wind [41]	385565	10000	6
prices [42]	34895	10000	61

features represent the weather temperature and humidity of Tetouan city, located in north Morocco. Therefore, the feature dimension was reduced to 9, and the target vector dimension increased to 3.

E More Details on Relevant Methods

E.1 Split Conformal Prediction

Given n i.i.d. training data points $\{(X_i, Y_i)\}_{i=1}^{n-1}$, SCP constructs a prediction set for the unknown Y_n using the observed test feature vector X_n as follows. First, it splits the n observed samples into a proper training set, indexed by \mathcal{I}_1 , and a calibration set, indexed by \mathcal{I}_2 . Then, the method proceeds by fitting a model \mathcal{M} on the proper training set, where the trained model is used to compute *non-conformity scores* on the calibration set, i.e., $\{S(\mathcal{M}(X_i), Y_i)\}_{i \in \mathcal{I}_2}$. Intuitively, the score function $S(\mathcal{M}(X_i), Y_i)$ measures the model's prediction error or a measure of goodness-of-fit, which can be the absolute residual error in regression tasks, the inverse of the predicted class probability in multi-class classification problems, or any of the clever scores proposed in [10, 29, 36, 49–55]. Lastly, SCP constructs the uncertainty set for a new test point:

$$C_{1-\alpha}^{\text{SCP}}(X_n) = \{y \in \mathcal{Y} : S(\mathcal{M}(X_n), y) \leq Q_{1-\alpha}(\{S(\mathcal{M}(X_t), Y_t)\}_{t \in \mathcal{I}_2})\},$$

where $Q_{1-\alpha}(\{S(\mathcal{M}(X_i), Y_i)\}_{i \in \mathcal{I}_2})$ is the $1 - \alpha$ quantile of the set $\{S(\mathcal{M}(X_i), Y_i)\}_{i \in \mathcal{I}_2}$. This base procedure can be easily altered to construct prediction intervals rather than sets [e.g., 33] and to control other statistical error rates beyond miscoverage [11, 56].

E.2 Adaptive Conformal Inference

The full description of ACI is summarized in Algorithm 2.

E.3 Online ACI

The method of ACI-Online we introduce here is a straightforward combination of *online sequential split conformal prediction* (OSSCP) [22] and ACI, which we consider as a powerful baseline method. OSSCP [22] is a recent calibration scheme that can be viewed as an online version of SCP. This is achieved by forming training and calibration sets that always contain consecutive data points, as such OSSCP can work with any online learning algorithm. While this approach is highly efficient, it is not guaranteed to satisfy the coverage requirement (1) if the i.i.d. assumption is violated. However, this limitation can be easily alleviated by combining OSSCP with ACI. Specifically, we suggest tuning the raw coverage level α_t according to the updating rule of ACI (3) and use the most recent samples to form a calibration set as in OSSCP. We visualize ACI-Online in Figure 2b, and provide its pseudo-code in Algorithm 3. Following these, one can see that the predictive model \mathcal{M}_t is updated online once a new sample is observed, however, it is not allowed to fit on the newest samples as these are dedicated only for calibration. As a consequence, ACI-Online may be slower to adapt to distributional shifts compared to Rolling CI, which is indeed confirmed by our experiments. The coverage guarantee of this method follows from Theorem 1 by defining:

$$f(X_t, \theta_t, \mathcal{M}_t) = \{y \in \mathcal{Y} : S(\mathcal{M}_t(X_t), y) \leq Q_{1+\theta_t}(\{S(\mathcal{M}_{t-n_2}(X_i), Y_i)\}_{i=t-n_2}^{t-1})\}.$$

E.4 Rolling CI with Calibration Set

We provide the pseudo-code of Rolling CI with cal in Algorithm 4.

Algorithm 2 ACI

Input:

Data $\{(X_t, Y_t)\}_{t=1}^T \subseteq \mathcal{X} \times \mathcal{Y}$, given as a stream, miscoverage level $\alpha \in (0, 1)$, a score function S , a calibration set size n_2 , a step size $\gamma > 0$, and an online learning model \mathcal{M} .

Process:

- 1: Initialize $\alpha_0 = \alpha$.
- 2: **for** $t = n_2, \dots, T$ **do**
- 3: Split the observed data $\{X_i, Y_i\}_{i=1}^{t-1}$ into a training set of size $t - 1 - n_2$, indexed by \mathcal{I}_1 and a calibration set of size n_2 , indexed by \mathcal{I}_2 .
- 4: Obtain a predictive model \mathcal{M}_t by fitting the initial one on the training set $\{X_i, Y_i\}_{i \in \mathcal{I}_1}$.
- 5: Construct a prediction set for the new point X_t :

$$\hat{C}_t^{\text{ACI}}(X_t) = \{y \in \mathcal{Y} : S(\mathcal{M}_t(X_t), y) \leq Q_{1-\alpha_t}(\{S(\mathcal{M}_t(X_i), Y_i)\}_{i \in \mathcal{I}_2})\}$$

- 6: Obtain Y_t .
- 7: Compute $\text{err}_t = \mathbb{1}\{Y_t \notin \hat{C}_t^{\text{ACI}}(X_t)\}$.
- 8: Update $\alpha_{t+1} = \alpha_t + \gamma(\alpha - \text{err}_t)$.
- 9: **end for**

Output:

Uncertainty sets $\hat{C}_t^{\text{ACI}}(X_t)$ for each time step $t = n_2, \dots, T$.

Algorithm 3 ACI-Online

Input:

Data $\{(X_t, Y_t)\}_{t=1}^T \subseteq \mathcal{X} \times \mathcal{Y}$, given as a stream, miscoverage level $\alpha \in (0, 1)$, a score function S , a calibration set size n_2 , a step size $\gamma > 0$, and an online learning model \mathcal{M} .

Process:

- 1: Initialize $\alpha_0 = \alpha$.
- 2: **for** $t = n_2, \dots, T$ **do**
- 3: Construct a prediction set for the new point X_t :

$$\hat{C}_t^{\text{ACI}}(X_t) = \{y \in \mathcal{Y} : S(\mathcal{M}_t(X_t), y) \leq Q_{1-\alpha_t}(\{S(\mathcal{M}_{t-n_2}(X_i), Y_i)\}_{i=t-n_2}^{t-1})\}.$$

- 4: Obtain Y_t .
- 5: Compute $\text{err}_t = \mathbb{1}\{Y_t \notin \hat{C}_t^{\text{ACI}}(X_t)\}$.
- 6: Update $\alpha_{t+1} = \alpha_t + \gamma(\alpha - \text{err}_t)$.
- 7: Fit the model \mathcal{M}_{t-n_2} on (X_{t-n_2}, Y_{t-n_2}) and obtain the updated model \mathcal{M}_{t-n_2+1} .
- 8: **end for**

Output:

Uncertainty sets $\hat{C}_t^{\text{ACI}}(X_t)$ for each time step $t = n_2, \dots, T$.

F Time-Series Conditional Coverage Metrics

F.1 Average Miscoverage Streak Length

Following Section 4, recall that the miscoverage streak length of a series of intervals $\{\hat{C}_t(X_t)\}_{T_0}^{T_1}$ is defined as:

$$\text{MSL} := \frac{1}{|\mathcal{I}|} \sum_{t \in \mathcal{I}} \min\{i : Y_{t+i} \in \hat{C}_{t+i}(X_{t+i}) \text{ or } t = T_1\},$$

where \mathcal{I} is a set containing the starting times of all miscoverage streaks:

$$\mathcal{I} = \left\{ t \in [T_0, T_1] : \left(t = T_0 \text{ or } Y_{t-1} \in \hat{C}_{t-1}(x_{t-1}) \right) \text{ and } Y_t \notin \hat{C}_t(X_t) \right\}.$$

Above, $[T_0, T_1]$ is the set of all integers between T_0 and T_1 .

To clarify this definition of the MSL, we now analyze the MSL in two concrete examples. Denote by “1” a coverage event and by “0” a miscoverage event, and consider a sequence of 15 observations. A

Algorithm 4 Rolling CI with cal

Input:

Data $\{(X_t, Y_t)\}_{t=1}^T \subseteq \mathcal{X} \times \mathcal{Y}$, given as a stream, miscoverage level $\alpha \in (0, 1)$, a score function S , a calibration set size n_2 , a step size $\gamma > 0$, and an online learning model \mathcal{M} .

Process:

1: Initialize $\alpha_0 = \alpha$ and a set of the previous conformity scores: $\mathcal{S}_{\text{cal}} = \emptyset$.

2: **for** $t = 1, \dots, T$ **do**

3: Construct a prediction set for the new point X_t :

$$\hat{C}_t^{\text{RCI-WC}}(X_t) = \{y \in \mathcal{Y} : S(\mathcal{M}_t(X_t), y) \leq Q_{1-\alpha_t}(\mathcal{S}_{\text{cal}})\}.$$

4: Obtain Y_t .

5: Compute the current conformity score: $s_t = S(\mathcal{M}_t(X_t), Y_t)$.

6: Add the current conformity score to the set: $\mathcal{S}_{\text{cal}} = \mathcal{S}_{\text{cal}} \cup \{s_t\}$.

7: Remove the oldest calibration point from the set: $\mathcal{S}_{\text{cal}} = \mathcal{S}_{\text{cal}} - \{s_{t-n_2}\}$.

8: Compute $\text{err}_t = \mathbb{1}\{Y_t \notin \hat{C}_t^{\text{RCI-WC}}(X_t)\}$.

9: Update $\alpha_{t+1} = \alpha_t + \gamma(\alpha - \text{err}_t)$.

10: Fit the model \mathcal{M}_t on (X_t, Y_t) and obtain the updated model \mathcal{M}_{t+1} .

11: **end for**

Output:

Uncertainty sets $\hat{C}_t^{\text{RCI-WC}}(X_t)$ for each time step $t \in \{1, \dots, T\}$.

method that results in the following coverage sequence:

$$1, 1, 1, 1, 1, \mathbf{0}, 1, \mathbf{0}, \mathbf{0}, 1, 1, 1, 1, 1,$$

has an $\text{MSL} = (2 + 1)/2 = 1.5$, and $\text{coverage} = 12/15 = 80\%$. By contrast, a method that results in the following sequence

$$1, 1, 1, 1, 1, 1, 1, 1, \mathbf{0}, \mathbf{0}, \mathbf{0},$$

has the same average coverage of 80% but much larger $\text{MSL} = 3/1 = 3$. This emphasizes the role of MSL : while the two methods cover the response in 12 out of 15 events, the second is inferior as it has, on average, longer streaks of miscoverage events.

We now compute the MSL of intervals constructed by the true conditional quantiles $\{C(X_t)\}_{t=T_0}^{T_1}$. By construction, these intervals satisfy:

$$\mathbb{P}(Y_t \in C(X_t) \mid X_t = x_t) = 1 - \alpha.$$

Therefore, $Z_t = \min\{i : y_{t+i} \in \hat{C}(X_{t+i}) \text{ or } t = T_1\}$ is a geometric random variable with success probability $1 - \alpha$. The average miscoverage streak length of the true quantiles is the mean of Z_t , which is:

$$\text{MSL} = \frac{1}{1 - \alpha} \underset{\alpha=0.1}{\approx} 1.111.$$

Therefore, having $\text{MSL} = 1$ is not necessarily equivalent to an optimal conditional coverage, as it indicates for undesired anti-correlation between two consecutive time steps: after a miscoverage event follows a coverage event with probability one. Consequently, we would desire to have $\text{MSL} = \frac{1}{1-\alpha}$, which is the MSL attained by the true conditional quantiles.

F.2 $\Delta\text{Coverage}$

Given a series of intervals $\{\hat{C}_t(X_t)\}_{T_0}^{T_1}$, their $\Delta\text{Coverage}$ is formulated as:

$$\Delta\text{Coverage} = \frac{1}{7} \sum_{i \in \{1, 2, \dots, 7\}} \left| \frac{1}{|D_i|} \sum_{t \in D_i} \mathbb{1}_{Y_t \in \hat{C}_t(X_t)} - (1 - \alpha) \right|,$$

where D_i is a set of samples that belong to the i -th day of the week.

G Constructing Prediction Sets in Classification Tasks

In this section, we show how to formulate a prediction set constructing function inspired by [36, 50], which is known to attain better conditional coverage than the function presented in Section 3.3. The idea is to initialize an empty prediction set and add class labels to it, ordered by scores produced by the model. We keep adding class labels until the total score exceeds $1 - \alpha$. Formally, the confidence set function is defined as:

$$f(X_t, \theta_t, \mathcal{M}_t) = \{\pi_1, \dots, \pi_k\}, \text{ where } k = \inf \left\{ k : \sum_{j=1}^k (\mathcal{M}_t(X_t, \pi_j)) \geq 1 - \varphi(\theta_t) \right\},$$

and π is the permutation of $\{1, 2, \dots, K\}$ sorted by the scores $\{\mathcal{M}_t(X_t, y) : t \in \mathcal{Y}\}$ from the highest to lowest. As for the stretching function φ , we recommend using $\varphi(x) = x$.